

Short-range Wireless Transmitter Using Mesoscopic Dielectric Cuboid Antenna in 300-GHz Band

Kazuki Yamada[#], Yuto Samura[#], Oleg Vladilenovich Minin^{S*}, Atsushi Kanno[^],
Norihiro Sekine[^], Junichi Nakajima⁺, Igor Vladilenovich Minin^{S*}, Shintaro Hisatake^{#1}

[#]Gifu University, Gifu, Japan,

^SNational Research Tomsk State University, Tomsk, Russia

^{*}Tomsk Polytechnical University, Tomsk, Russia

[^]National Institute of information and Communication Technology, Tokyo, Japan

⁺SoftBank, Tokyo, Japan

¹hisatake@gifu-u.ac.jp

Abstract — We demonstrate short-range terahertz (THz) wireless transmission using a high-gain and low-profile dielectric cuboid antenna (DCA) in the 300 GHz band. The compact DCA will support high-speed mobile user equipment (UE) in the next generation. The simple rectangular structure enables easy installation and we configure the current design to a standard waveguide (WR-3.4). The DCA was developed with polytetrafluoroethylene and has dimensions of $1.36\lambda \times 1.36\lambda \times 1.79\lambda$ ($1.36 \text{ mm} \times 1.36 \text{ mm} \times 1.79 \text{ mm}$ at 300 GHz). Antenna patterns of the DCA at 300 GHz were evaluated using a near-field electro-optic sensing technique. The far-field pattern calculated from the measured near-field pattern showed good agreement with simulation results. The calculated antenna gain was 15.5 dBi. The wireless transmitter configured with the developed DCA has been demonstrated in the 300 GHz band. The resultant data rate with amplitude-shift keying of 17.5 Gbit/s was achieved at transmission distance of 79 mm.

Keywords — mesoscopic dielectric cuboid antenna, low-profile antenna, terahertz wireless communication, electro-optic sensing.

I. INTRODUCTION

Recent high-performance UE evolution requires ultra-fast external radio link support their processor performance and storage capacity. Terahertz (THz) bands ($>0.1 \text{ THz}$) in the range 252–325 GHz allocated by the new IEEE 802.15.3d standard [1] is the expected frequency to support these UE demands under the next generation wireless networks. The THz bands are expected not only for backhaul and fronthaul [2], [3], but also for short-range communication [4], hence other RF sub-system studies are being carried out on the development of THz wave integrated circuits [5], [6] and transceiver systems [2] to achieve the data rate of more than 100 Gbps [7]–[10]. These new higher frequency bands beyond 5G will support indispensable functions such as download large volume video contents, OS upgrade, system back-up and new emerging applications.

In wireless communication systems, antennas are a key device to improve system capability and/or to enhance transmission distance. In addition, UEs equip 5G frequency

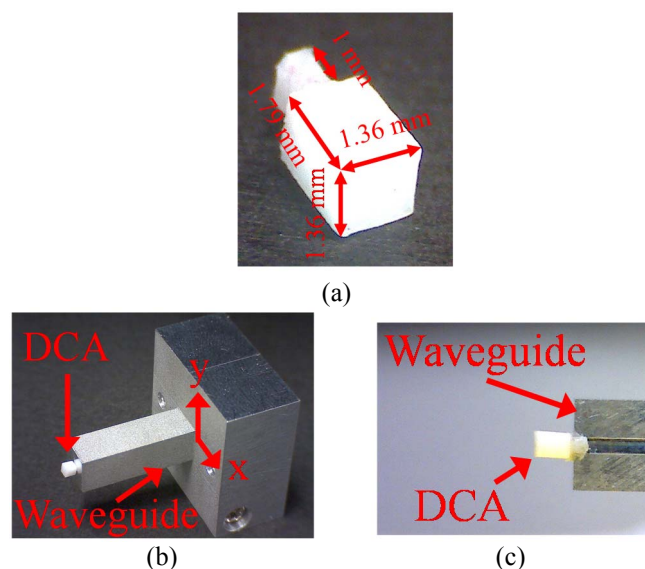


Fig. 1. (a) Photograph of the fabricated DCA. Protrusion part is connected to the WR-3.4 standard waveguide. (b) DCA connected to the open-ended waveguide. (c) Enlarged view of the connection part in (b)

band does not have much space left for additional antenna. Under the condition, the rectangular DCA could become an optimal solution. The antenna widely utilized in THz wireless communication is the horn antenna, which has the characteristics of broad bandwidth, easy connection to a waveguide, and moderate antenna gain [11]–[13]. For instance, a step-profiled corrugated horn antenna ($3.2\lambda \times 2.8\lambda \times 2.7\lambda$) with a typical antenna gain of 18 dBi has been demonstrated in the 300 GHz band [14]. To take advantage of not only the wide bandwidth but also the short wavelength of the THz wave carrier, minimizing antenna dimensions while maintaining directivity is desirable. A mesoscopic dielectric cuboid antenna (DCA) [15] based on the terajet effect [16], [17], with larger antenna gain than the horn antenna for the same antenna aperture size and throat length [15], is proposed with small dimensions. The basic characteristics were

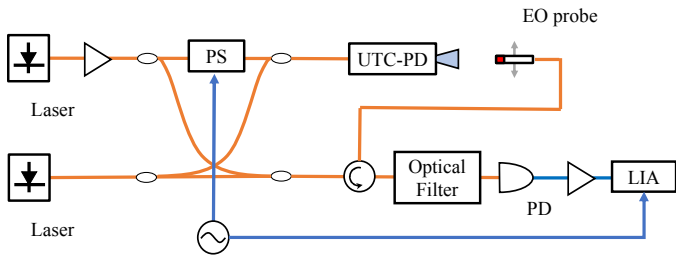


Fig. 2. The experimental setup for the near-field visualization. PS is Phase shifter and PD is photodiode. The near-field distribution was measured with electro-optic (EO) probe.

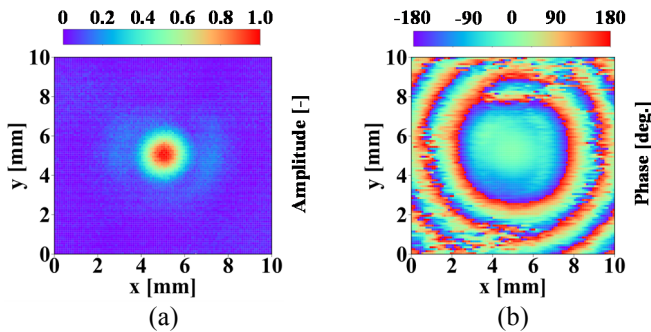


Fig. 3. Measured (a) amplitude and (b) phase distribution at the shadow surface of DCA. The amplitude distribution is normalized to its maximum value.

experimentally validated at 24 GHz, indicating higher gain with a low-profile feature.

In this paper, we configure a THz wireless transmitter using the high-gain and low-profile DCA in the 300 GHz band. The developed DCA is made of polytetrafluoroethylene (PTFE) and is easily connected to a standard waveguide. The structure is cubic, and the size is in the mesoscopic scale: $1.36\lambda \times 1.36\lambda \times 1.79\lambda$ ($1.36 \text{ mm} \times 1.36 \text{ mm} \times 1.79 \text{ mm}$ for 300 GHz). We measured the near-field electromagnetic-field distribution of the THz waves radiating from the DCA, and characterized the far-field patterns based on near-field to far-field transformation. Using the DCA as a transmitter (Tx) antenna, we evaluated short-range THz wireless transmission at a data rate of 17.5 Gbit/s with amplitude-shift keying (ASK) modulation format.

II. CHARACTERIZATION OF THE DCA

Fig. 1a shows the structure of the DCA, which consists of a cuboid antenna and a protrusion (1 mm length) that connect to a standard waveguide. We selected PTFE as the material for DCA, which has a dielectric constant and loss tangent of 2.0 and 11×10^{-4} at 300 GHz, respectively. The DCA was manufactured in a machine milling. Fig. 1b and 1c shows a photograph of the DCA connected to an open-ended waveguide (WR-3.4). The connection method between the waveguide and DCA is simply insertion. Fig. 2 shows the experimental setup for near-field measurements. The electro-optic (EO) probe consists of an organic EO crystal ($0.5 \text{ mm} \times 0.5 \text{ mm} \times 0.5 \text{ mm}$) with a relative dielectric constant of 5.76 at

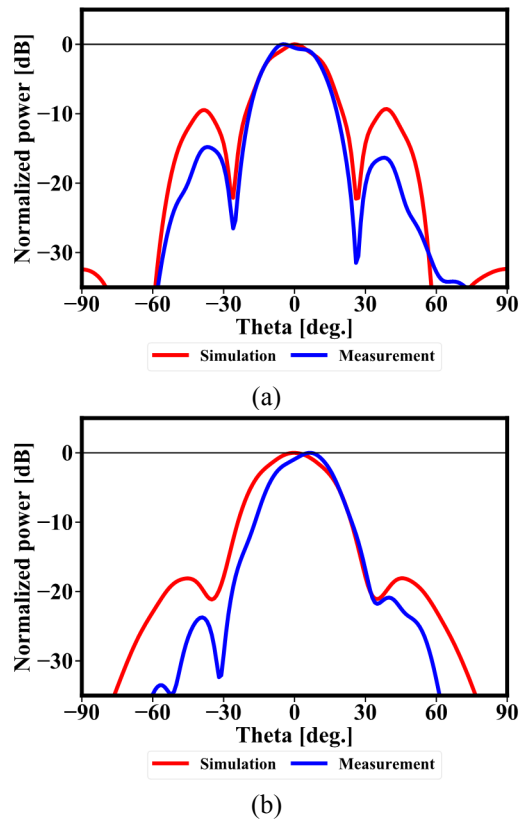


Fig. 4. Far-field pattern calculated from the measured near-field distribution. The near-field to far-field transformation is conducted using CST studio suite. (a) E-plane. (b) H-plane.

300 GHz, graded-index lens, and polarization-maintaining optical fiber. The nonpolarimetric frequency down-conversion technique [18] and self-heterodyne technique [19] were used for the measurements. In the experiment, the 300 GHz signal was generated by a uni-traveling-carrier photodiode (UTC-PD). The output power for the measurements was approximately -16 dBm.

Fig. 3 shows the measured amplitude and phase distribution. The distance between the antenna surface and measurement plane was 2 mm. The measurement area was $10 \text{ mm} \times 10 \text{ mm}$. From the measured near-field distribution, we calculated the far-field distribution as shown in Fig. 4, and compared them with the simulated results. The simulation was conducted using CST Studio Suite software (finite integration method). Fig. 4a and 4b show the far-field distribution for the E-plane and H-plane, respectively. The far-fields were normalized to their maximum value. The full width at half maximum (FWHM) of the measured far-field pattern for the E-plane and H-plane were 23° and 24° , respectively. The FWHM of the far-field pattern calculated using the simulated near-field pattern for the E-plane and H-plane was 25° and 29° , respectively. The experimental results showed good agreement with the simulated results. The calculated antenna gain was 15.5 dBi.

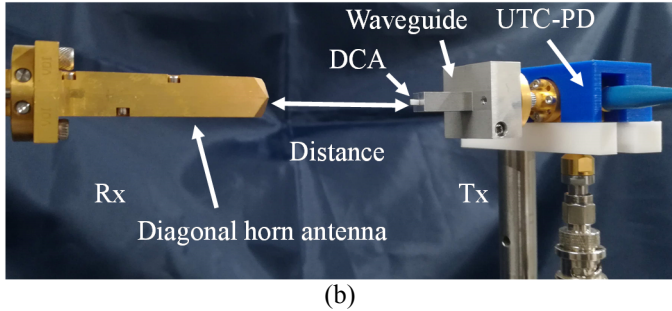
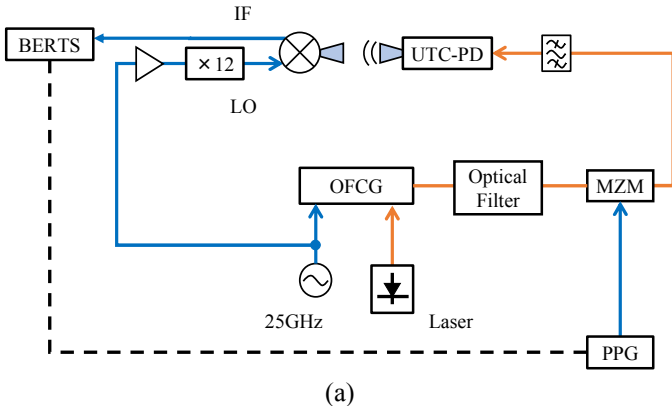


Fig. 5. (a) Block diagram of the experimental setup for the wireless transmission based on ASK modulation. (b) DCA was used on the Tx and diagonal horn antenna was used on the Rx.

III. TRANSMITTER PERFORMANCE EVALUATION

Fig. 5a shows the experimental setup for transmitter (Tx) evaluation. The transmitter was based on photonics technology, whereas the receiver was based on electronics. An optical two-tone signal utilized as an optical local oscillator (LO) signal was generated by an optical frequency comb generator (OFCG), and an optical filter suppressed unnecessary components from the OFCG signal. The OFCG was driven by an electrical LO source at a frequency of 25 GHz with resultant comb spacing of 25 GHz. The carrier frequency was set to 300 GHz. The optical carrier was modulated with an optical Mach-Zehnder modulator by an on-off keying (OOK) signal, which was generated by a pulse pattern generator (PPG). The modulated optical two-tone signal with frequency separation of 300 GHz was converted into the THz signal with the UTC-PD used as an optical-to-electrical converter. In the setup, BERTScope (Tektronix, BSA175C) was utilized as the PPG and bit-error-rate tester (BERT). The test pattern of the PPG and BERT is a pseudo-random bit sequence with a length of $2^{15}-1$ and a data rate of up to 17.5 Gbit/s. The UTC-PD converted the optical OOK signal into the THz ASK. The generated THz signal was emitted from the DCA directly attached to the waveguide device shown in Fig. 5b. The power emitted was approximately -18 dBm. In the receiver side (Rx), the signal supplied from the LO synthesizer was multiplied by a factor of 12 and mixed with the RF signal received by the diagonal horn antenna. It should be noted that the LO signal was supplied by

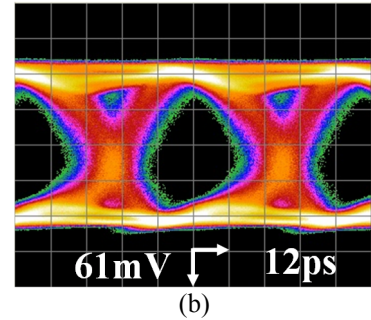
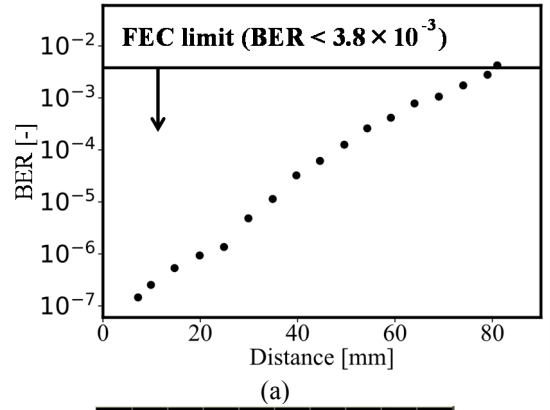


Fig. 6. (a) BER characteristics when DCA is Tx and diagonal horn antenna is Rx. (b) Eye diagram when BER was the smallest.

the synthesizer used for the OFCG on the Tx side. This is because of the evaluation of the DCA antenna without the phase noise fluctuations of the LOs in the transmission system. The amplified baseband signal was mixed down by the harmonic mixer set after the horn antenna was evaluated using BERTScope to obtain the bit error rates (BERs) and eye diagrams.

Fig. 6a shows the dependence of BER on the distance between the Tx DCA and Rx horn antenna facets. The BER of 1.46×10^{-7} was achieved at a distance of 7 mm; the demodulated eye diagram at that distance is also shown in Fig. 5b. A 7%-overhead continuously-interleaved Bose Chaudhuri and Hocquenghem code with an outer forward error correction limit of 3.8×10^{-3} [20] was achieved when the distance was 79 mm. Therefore, the DCA can be available for high-data-rate short-range wireless systems.

IV. CONCLUSION

We designed and developed a high-gain and low-profile DCA in the 300 GHz band for short-range wireless transmission. The dimensions of the DCA were in mesoscopic scale: $1.36\lambda \times 1.36\lambda \times 1.79\lambda$ (1.36 mm \times 1.36 mm \times 1.79 mm at 300 GHz). The antenna patterns obtained by near-field electro-optic sensing had good agreement with the result obtained by numerical simulation. The feature of easy connectivity to the standard waveguide helps in realizing a short-range and small-profile wireless Tx with antenna gain of 15.5 dBi. The proposed mesoscopic DCA is suitable for THz inter-chip and board-to-board communication in data centers.

ACKNOWLEDGMENT

This research is partially supported by funding from Horizon 2020, the European Union's Framework Program for Research and Innovation under grant agreement No. 814523. ThoR has also received funding from the National Institute of Information and Communications Technology in Japan. The work by I. V. Minin and O. V. Minin was carried out within the framework of the Tomsk Polytechnic University Competitiveness Enhancement Program and was partially supported by the RFBR Grant No. 20-57-S52001.

REFERENCES

- [1] "IEEE Standard for High Data Rate Wireless Multi-Media Networks Amendment 2: 100 Gbps Wireless Switched Point-to-Point Physical Layer," IEEE-SA Standards Board Std.
- [2] I. Dan, G. Ducournau, S. Hisatake, P. Szriftgiser, R.-P. Braun, and I. Kallfass, "A Terahertz Wireless Communication Link Using a Superheterodyne Approach," *IEEE Transactions on Terahertz Science and Technology*, Nov. 2019.
- [3] T. Kürner, T. Kawanishi, R.-P. Braun, I. Dan, G. Ducournau, A. Hirata, S. Hisatake, L. John, P. Jurcik, I. Kallfass, K. Kondou, Y. Leiba, B. Napier, S. Rey, E. Sasaki, and P. Szriftgiser, "Terahertz Wireless Transport Links for Beyond 5G Networks," *IEEE Vehicular Technology Magazine*, Apr. 2019.
- [4] Y. Nakasha, S. Shiba, Y. Kawano, and T. Takahashi, "Compact Terahertz Receiver for Short-range Wireless Communications of Tens of Gbps" *Fujitsu scientific & technical journal* 53(2):9-14, Feb. 2017
- [5] I. Dan, B. Schoch, G. Eren, S. Wagner, A. Leuther and I. Kallfass, "A 300 GHz MMIC-based quadrature receiver for wireless terahertz communications," 2017 42nd International Conference on Infrared, Millimeter, and Terahertz Waves (IRMMW-THz), pp. 1-2, 2017.
- [6] C. Grötsch, A. Tessmann, A. Leuther and I. Kallfass, "Ultra-wideband quadrature receiver-MMIC for 240 GHz high data rate communication," 2017 42nd International Conference on Infrared, Millimeter, and Terahertz Waves (IRMMW-THz), pp. 1-2, 2017.
- [7] I. Kallfass, I. Dan, S. REY, P. Harati, J. Antes, A. Tessmann, S. Wagner, M. Kuri, R. Weber, H. Massler, A. Leuther, T. Merkle, and T. Kürner, "Towards MMIC-based 300 GHz indoor wireless communication systems," *IEICE Transactions on Electronics*, vol. E98.C, No. 12, pp. 1081–1090, Dec. 2015.
- [8] T. Kürner, T. Kawanishi, R.-P. Braun, I. Dan, G. Ducournau, A. Hirata, S. Hisatake, L. John, P. Jurcik, I. Kallfass, K. Kondou, Y. Leiba, B. Napier, S. Rey, E. Sasaki, and P. Szriftgiser, "Terahertz Wireless Transport Links for Beyond 5G Networks," *IEEE Vehicular Technology Magazine*, Apr. 2019.
- [9] T. Harter, M. M. H. Adib, S. Wolf, S. Muehlbrandt, M. Weber, M. Blaicher, F. Boes, H. Massler, A. Tessmann, S. Nellen, T. Goebel, J. Giesekus, M. Walther, T. Zwick, W. Freude, S. Randel, and C. Koos, "Wireless Multi-Subcarrier THz Communications Using Mixing in a Photoconductor for Coherent Reception", *IEEE Photonics Conference*, 147-148, 2017.
- [10] H. Son, D. Kim, K. Song, J.-H. Cho, and J.-S. Rieh "A 300-GHz Integrated Transmitter based on InP HBT Technology", 2018 Asia-Pacific Microwave Conference, 524-526, Jan. 2019.
- [11] S. Hisatake, M. Fujita, H. H. Nguyen Pham, K. Tsuruda, S. Kuwano, J. Terada, "Millimeter-Wave and Terahertz-Wave Applications Enabled by Photonics," *IEEE Journal of Quantum Electronics*, vol. 52, Issue 1, Dec. 2015.
- [12] T. Nagatsuma, S. Horiguchi, Y. Minamikata, Y. Yoshimizu, S. Hisatake, S. Kuwano, N. Yoshimoto, J. Terada, and H. Takahashi, "Terahertz wireless communications based on photonics technologies," *Optics Express*, vol. 21, No. 20, pp. 23736–23747, 2013.
- [13] T. Tajima, H. Song, and M. Yaita, "300-GHz microstrip-to-waveguide transition on a polyimide substrate integrated with an LTCC substrate integrated waveguide," *IEICE Transactions on Electronics*, vol. E98.C, No. 12, pp. 1120–1127, 2015.
- [14] T. Tajima, H. Song, K. Ajito, M. Yaita, and N. Kukutsu "300 GHz Step profile d Corrugated Horn Antennas Integrated in LTCC," *IEEE Transactions on Antennas and Propagation*, vol. 62, No. 11, pp. 5437-5444, Aug. 2014
- [15] Y. Samura, K. Horio, V. Antipov, S. Shipilov, A. Ereemeev, O. V. Minin, I. V. Minin, and S. Hisatake, "Characterization of Mesoscopic Dielectric Cuboid Antenna at Millimeter-Wave Band," *IEEE Antennas and Wireless Propagation Letters*, vol. 18, No. 9, pp.1828-1832, Sep. 2019.
- [16] V. Pacheco-Peña, M. Beruete, I. V. Minin, and O. V. Minin. "Terajets produced by 3D dielectric cuboids," *Applied Physics Letters*, vol. 105, No. 8, Aug. 2014.
- [17] H. H. Nguyen Pham, S. Hisatake, I.V. Minin, O.V. Minin, T. Nagatsuma. "Three-dimensional direct observation of Gouy phase shift in a terajet produced by a dielectric cuboid," *Applied Physics Letters*, 108(19) 2016
- [18] S. Hisatake, H. H. Nguyen Pham, and T. Nagatsuma, "Visualization of the spatial-temporal evolution of continuous electromagnetic waves in the terahertz range based on photonics technology," *Optica*, vol. 1, no. 6, pp. 365–371, 2014.
- [19] S. Hisatake, H. Nakajima, H. H. Nguyen Pham, H. Uchida, M. Tojyo, Y. Oikawa, K. Miyaji, and T. Nagatsuma, "Mapping of electromagnetic waves generated by free-running self-oscillating devices," *Scientific Reports*, vol. 7, No. 1, Jun. 2017.
- [20] F. Chang, K. Onohara, and T. Mizuochi, "Forward error correction for 100 G transport networks," *IEEE Communications Magazine*, vol. 48, no. 3, pp. S48–S55, Mar. 2010.